Journal of Materials Chemistry C

Accepted Manuscript

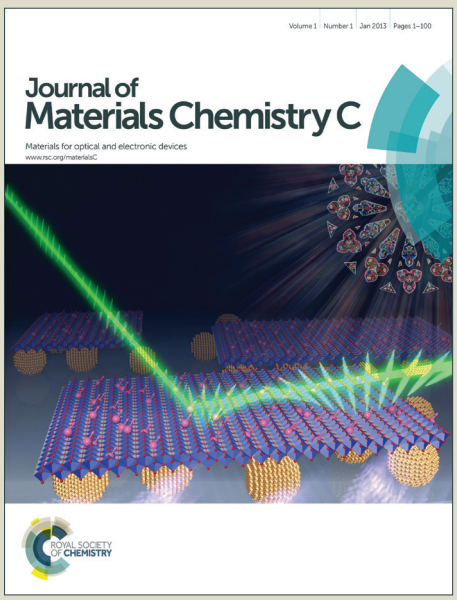

ROYAL SOCIETY OF CHEMISTRY

www.rsc.org/materialsC

Journal Name

RSCPublishing

ARTICLE

Ethanolamine-assisted synthesis of size-controlled indium tin oxide nanoink for solution deposited transparent conductive film with low annealing temperature

Cite this: DOI: 10.1039/xoxxoooooox

Received ooth January 2012,
Accepted ooth January 2012

DOI: 10.1039/xoxxoooooox

www.rsc.org/

Zheng Chen*, Xichao Qin, Teng Zhou, Xinzhou Wu, Shuangshuang Shao, Meilan Xie, Zheng Cui*

Highly conductive indium tin oxide (ITO) nanocrystals and inks have been synthesized by solvothermal dehydration condensation of metal hydroxide in combination with in-situ ethanolamine capping. It is found that the addition of ethanolamine can effectively reduce the size of nanocrystals and chemically modify their surfaces. The synthesized ITO nanocrystals can be well dispersed in ethanol with high solid content and the suspension is stable for days. Such small-molecule capped ITO suspension has been used as a conductive ink to make transparent conductive films by spin coating. Furthermore, a water washing step has been introduced in the ITO film preparation process to improve its conductivity, resulting in low resistivity of $8.9\times10^{-3}\Omega$•cm after 2 hours annealing at 300°C in mixed Ar and H_2 atmosphere.

Introduction

Indium tin oxide (ITO) is the most representative transparent conductive oxides (TCO) which have been widely used for transparent electrodes in flat panel display, organic light emitting diodes, photovoltaics, touch screens, *etc*.[1] Conventionally, ITO electrodes are produced via vacuum deposition methods such as magnetron sputtering [2] and evaporation, followed by photolithography and etching processes. Recently, solution processes such as spin-coating and inkjet printing have attracted extensive interests due to the advantages in process simplification, low cost, large-area manufacturing and high-throughput, *etc*.[3-5] These solution processes, however, require high quality inks for film deposition.[4]

Metal oxide inks currently available can be divided into two categories: (1) metal compound solution-type ink, also called as metal-organic decomposition (MOD) ink; (2) nanoparticle suspension ink (nanoink).[5] Recently, considerable progresses have been made in MOD ink for low temperature processed transparent oxide semiconductor (TOS) film. However, few of them are suitable for TCO films with reasonable conductivity.[6] The difference is the much higher mobility and free electron concentration required for TCO film than for TOS film, which is generally achieved through high processing temperature to improve crystallinity and effective doping. The direct use of crystallized metal oxide nanoparticles can avoid the high temperature and doping which are required for conversion of chemical precursor into M-O-M bond (M is metal atom) in the case of MOD ink. Therefore, nanocrystal-based inks are promising for low temperature processing of TCO film. Moreover, nanocrystal inks are easier to form thick films compared to the MOD ink.[7-9]

It is known that the conductivity of film deposited from nanocrystal-based inks depends on the property of crystallized nanoparticles and the interfacial resistance between nanoparticles.[10, 11] To prevent aggregation in suspension, the surfaces of nanoparticles have to be modified with organic ligands. The long chains of ligand can provide strong steric hindrance which is good for the stable suspension of nanoparticles. However, the electrically insulating ligands hinder the charge transport, resulting in low carrier mobility.[12] Though it is preferable to use small molecular capping ligand to enhance the interfacial charge transport property of nanoparticles.[12-14], the downside is the difficulty to achieve stable nanocrystal suspension using small molecular capping ligand due to the weak steric hindrance. A promising strategy is to obtain high capping efficiency by *in-situ* capping the nanoparticle during the synthesis process, because the fresh surfaces of nanoparticles have high reactivity. However, such synthesis of ITO nanocrystals with controlled morphology, size, high crystallinity and effective doping is still a challenge, due to self-purification in semiconductor nanocrystal [15, 16] and capping agent effect[17].

In the present work, a novel synthesis process was designed to prepare ITO nanoink by *in-situ* ethanolamine (MEA) capping. Small-molecule ethanolamine is a classic stabilization agent widely used in conventional metal salt solution, because of its

excellent metallic chelating activity.[18, 19] It was found that the addition of ethanolamine can effectively reduce the nanocrystal size and improve their dispersion properties simultaneously. The capped ITO ink was used to deposit transparent conductive film by spin coating process. A water washing process was also introduced after film deposition to get rid of the surface capping agent to improve the film conductivity. ITO films of high transparency (90%) exhibited low resistivity of 8.9×10^{-3} Ω·cm after 2 hours annealing at 300°C in mixed Ar and H_2 atmosphere.

Experimental

Chemicals

All chemicals were used as received. Indium chloride tetrahydrate ($InCl_3{\cdot}4H_2O$, Reagent-grade), tin (IV) chloride pentahydrate ($SnCl_4{\cdot}5H_2O$), ethanolamine ($HO(CH_2)_2NH_2$, MEA), aqueous ammonia and anhydrous ethanol (C_2H_5OH) were purchased from Sinopharm Chemical Reagent Co, Ltd.

Preparation of ITO nanoparticles and ink

$InCl_3$ and $SnCl_4$ were dissolved in deionized water with the In:Sn molar ratio of 95: 5. Aqueous ammonia was added into the solution until the pH value was adjusted to 8~9. After washing with water and ethanol alternately for several circles to eliminate the excess ions, the resulting white precipitate was dispersed in ethanol or the mixture solvent of ethanolamine/ethanol with 0.14mol/L metal atom (In+Sn) concentration and loaded into autoclaves for thermal treatment. In the experiment, the ethanolamine concentrations were used: 0, 0.014, 0.14, 1.4 and 14mol/L. After thermal treatment at 250°C for 24h, the ITO nanocrystals were obtained and washed by rinsing in ethanol and centrifugation (8000 rpm, 10 min) alternately for 3 times. The washed ITO nanoparticles can be dispersed well into ethanol with weight ratio up to 10%, to serve as "ink" for further film preparation.

Solution deposition of ITO films

The above ITO inks were spin-coated at 1000 rpm for 60s onto alkali-free glass, and the ITO nanoparticle films were pre-dried at 180°C for 60s under air. Further, the final ITO films were annealed under air or Ar+7.5%H_2 atmosphere for 2h at the desired temperatures. For some samples, an additional water-washing step, immersing ITO film in water for 10min, was performed just after the spin-coating and drying, followed by another drying and the annealing step.

Characterization

The crystalline structure and morphology of the nanocrystals were investigated by powder X-ray diffraction (XRD, Bruker AXS D8 Advance, Cu kα) and transmission electron microscopy (TEM, FEI Tecnai G2 S-twin). Thermal behavior of the ITO product was monitored by thermogravimetry-differential scanning calorimetry (TGA-DSC, METTLER TOLEDO TGA/DSC1). The metal compositions of ITO nanoparticles were determined by Inductively Coupled Plasma Optical Emission Spectrometer (ICP, Thermo iCAP6300) measurement. The surface and cross-sectional morphology of ITO films were observed using scanning electron microscopy (SEM, Hitachi S-4800). The film thicknesses were determined with the SEM image and the measurement of Step profiler (Veeco, Dektak 150). The dispersion of ITO suspension was characterized using dynamic light scattering (DLS, MS2000). Sheet resistivity measurements of the ITO films were conducted by a 4-points technique on a Keithley 4200-SCS parameter analyzer. Transmittance of the ITO film on glass substrates was measured by a PerkinElmer Lambda 750 UV−Vis absorption spectrophotometer.

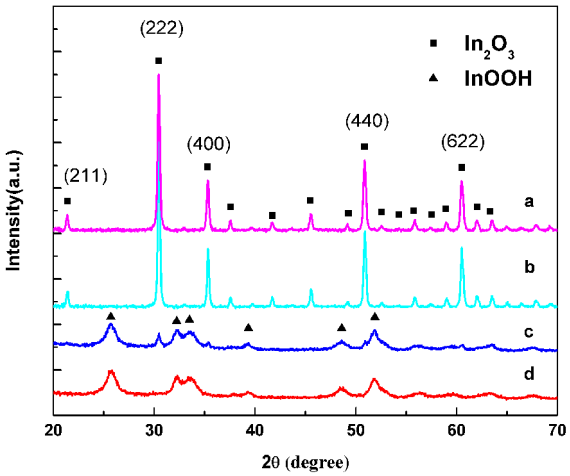

Fig.1 XRD patterns of products synthesized without ethanolamine at different temperatures: (a) 250°C; (b) 240°C; (c) 230°C; (d) 220°C for 24h.

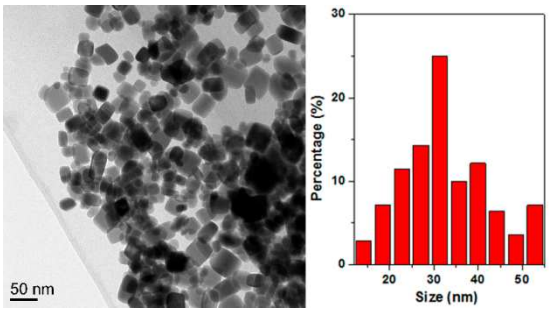

Fig.2 TEM image and the size (side length) distribution of ITO nanocrystals obtained at 250°C for 24h.

Results and Discussion

Dehydration condensation of indium and tin hydroxide in ethanol was employed for the synthesis of ITO nanocrystals in autoclaves which enabled reaction at temperature higher than boil point of solvent. Figure 1 presents the XRD patterns of products synthesized at different temperatures. At low temperatures (220-230°C), the products are whitish and have XRD peaks assigned to rhombohedra structure of indium oxyhydroxide (InOOH). When the reactive temperatures increased to 240-250°C, the obtained powders exhibited XRD peaks of pure In_2O_3 cubic bixbyite structure and no Sn species such as SnO_2 were observed, suggesting the formation of ITO. Furthermore, the deep blue color of products confirmed the successful Sn doping in ITO nanocrystals, because Sn^{4+} dopants provided free electrons which were responsible for the surface plasmon resonance in the near-infrared region that gives the

powder its blue color [13, 20]. Figure 2 shows the TEM image and size distribution of the ITO nanocrystals obtained at 250°C. The nanocrystals were cubic shape with side length range of 10-60nm. Different temperatures (240-250°C) and times (3-24h) were also investigated with negligible change in shapes and sizes.

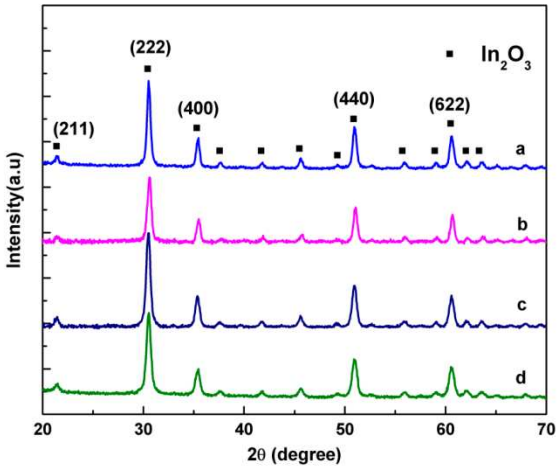

Fig.3 XRD patterns of particles synthesized at 250°C for 24 h at different ethanolamine concentrations: (a) 0.014mol/L; (b) 0.14mol/L; (c) 1.4mol/L and (d) 14mol/L.

It has been proven that the introduction of capping agent during the growth of nanocrystals is a good strategy to achieve the effective surface capping for subsequent dispersion in liquid[21-23]. Ethanolamine as a bidentate ligand has an amino group and a hydroxyl group, both of which have ability to coordinate metal atoms. They can act as stabilizing and chelating agents in metal salt alcohol solution to improve the solubility of precursor salts and the stability of solution against hydrolysis of the salts [18, 24-26]. It has also been found previously that ethanolamine acted as a structure-directing agent for the growth of different one dimentional nanostructures[27], due to the chelating. Ethanolamine is therefore introduced to the synthetic process by us to *in-situ* cap the ITO nanoparticles.

Figure 3 is XRD patterns of nanoparticles synthesized at 250°C for 24h at different ethanolamine concentrations. All of the products have a blue color and exhibited the XRD peaks of pure In_2O_3 cubic bixbyite structure, suggesting the formation of ITO nanocrystals. Moreover, no apparent change in metal ratio of the ITO nanoparticles was observed using ICP measurement whether with or without ethanolamine. All of ITO products have In/Sn ratios close to that of the initial metal salt precursor. Applying the Scherrer equation on the (400) peaks in Fig.1c and Fig.3, the average crystallite sizes are about 38.6, 24.1, 21.9, 20.1 and 18.3nm when the ethanolamine concentration are 0, 0.014, 0.14, 1.4 and 14mol/L, respectively. TEM images in Fig. 4 also exhibit that the sizes of ITO nanocrystals decrease with the increase of ethanolamine concentration in synthesis. It is well known that the addition of capping agent during synthetic reaction would simultaneously influence nanocrystal growth.[17]

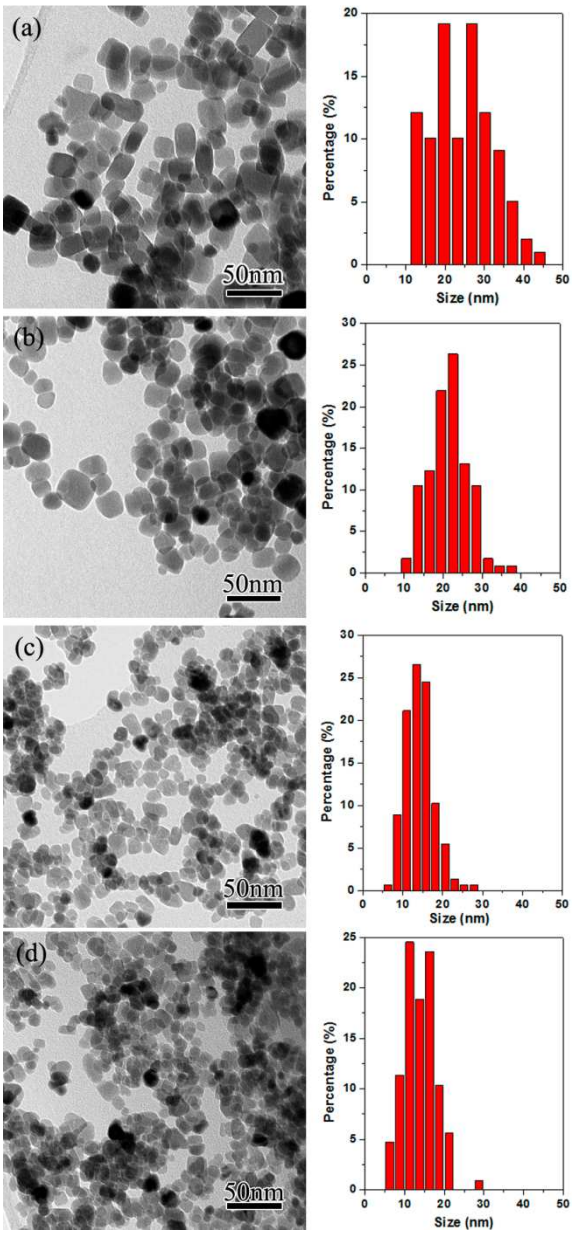

Fig.4 TEM images and the size (side length) distribution histograms of nanoparticles synthesized at 250°C for 24 h at different ethanolamine concentrations: (a) 0.014mol/L; (b) 0.14mol/L; (c) 1.4mol/L and (d) 14mol/L.

The phase transformation of metal hydroxide precursors have been investigated extensively and used for preparation of metal oxide nanocrystals including TiO_2[28], ITO[10] and In_2O_3[29]. According to the previous reports[29-32], indium hydroxide ($In(OH)_3$) would like to transform to InOOH at lower temperature while further evolve into In_2O_3 at higher temperature. Usually, InOOH would transform to rhombohedral In_2O_3, under ambient pressure and at moderate temperature. However, in our experiments, cubic phase of ITO was obtained though rhomboheral InOOH was observed at lower temperature. Similar results have been observed in some researches involving solvothermal phase transformation and due to a

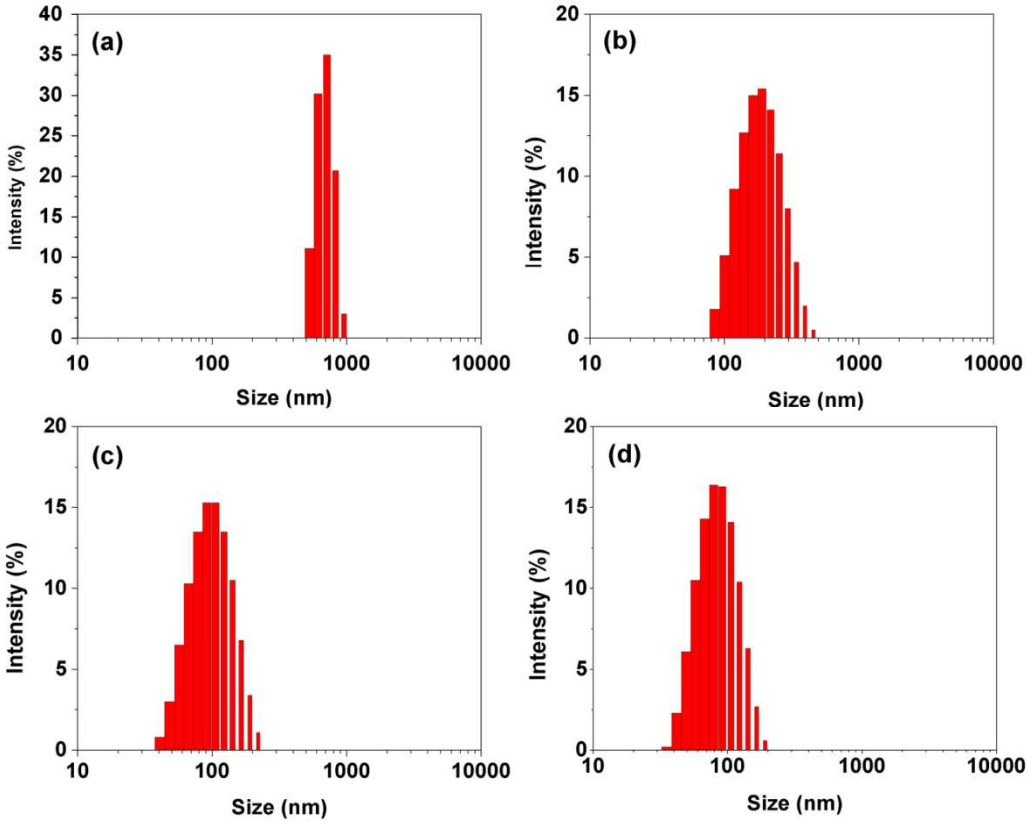

Fig. 5 DLS diameter size distribution histograms of ITO nanoparticles in ethanol suspension with different ethanolamine concentrations: (a) 0.014mol/L; (b) 0.14mol/L; (c) 1.4mol/L and (d) 14mol/L.

dissolution-recrystallization mechanism[29]: the rhombohedral InOOH decompose and dissolve in the solution, followed by the nucleation and growth of cubic structure In_2O_3 (here is ITO). Based on the theory proposed by LaMer and co-workers[33], higher concentration dissolution of metal species is beneficial for formation of more nuclei, resulting in smaller nanocrystals. Herein, the ethanolamine improved the solubility of metal species through chelating, leading to the formation of smaller nanocrystals.

To prepare ITO inks, the ITO nanoparticles synthesized at different ethanolamine concentrations were re-dispersed in ethanol after a centrifugation washing. Figure 5 shows the DLS size distributions of ITO nanoparticles in ethanol suspensions. The secondary particle sizes are larger than those of primary nanoparticles (TEM observation), indicating somewhat aggregation in the inks. High ethanolamine concentration

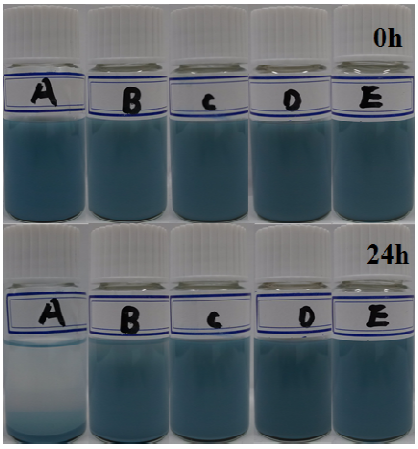

Fig. 6 ITO suspension in ethanol at 0 h and 24h under synthesis condition of 0 mol/L (a); (b) 0.014 mol/L; (c) 0.14 mol/L; (d) 1.4 mol/L; (e) 14 mol/L ethanolamine.

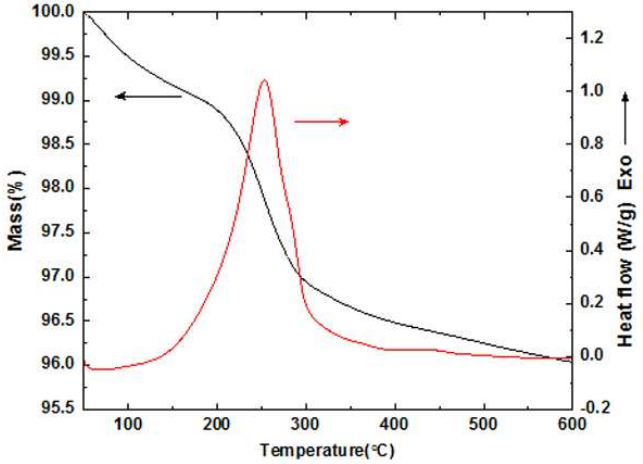

Fig. 7 The TGA-DSC measured in air of the dried ITO nanoparticles synthesized with 14mol/L ethanolamine.

Table 1 Electrical properties of ITO nanoparticle films annealed under different conditions

Annealing and Time	Temperature	Ambient	Water washing	Sheet resistance (Ω/sq)	Thickness (nm)	Resistivity (Ω·cm)
150°C 2h		Air	No	1.5×10^{6}	253	38
200°C 2h		Air	No	4.0×10^{5}	258	10.3
300°C 2h		Air	No	9.5×10^{3}	189	0.18
200°C 2h		Ar and 7.5% H_2	No	8.0×10^{4}	236	1.9
300°C 2h		Ar and 7.5% H_2	No	570	185	1.0×10^{-2}
200°C 2h		Ar and 7.5% H_2	Yes	9.0×10^{3}	226	0.2
300°C 2h		Ar and 7.5% H_2	Yes	466	191	8.9×10^{-3}

resulted in small secondary particle size of ITO nanoparticles in inks. The ITO suspensions prepared in higher concentration of ethanolamine also exhibited better suspension stability, as shown in Fig.6. In the case of 14mol/L ethanolamine, the ITO suspension (~10wt%) did not produce apparent precipitates over days. The dispersion improvement could be ascribed to the ethanolamine capping on the surface of ITO nanoparticles. Figure 7 showed the TGA-DSC measurement of ITO nanoparticles synthesized in 14mol/L ethanolamine. DSC curve shows an exothermic process in the range of 150~300°C which belongs to the thermal decomposition of MEA. Correspondingly, the TG curve indicated that most weight loss of ITO nanoparticles took place between 200~300°C, which was far higher than the boil points (~170°C) of ethanolamine. It suggested that the ethanolamine capping on nanoparticles was not simple physisorption but MEA-metal chelating.

The ITO inks were used to deposit ITO films on glass substrates by spin coating, followed by annealing to make films conductive. The film thicknesses were adjusted to ~200nm by varying the concentrations of inks. The results indicated that the film conductance improved with increased ethanolamine concentration applied in synthesis. After annealing at 300°C in air, film conductivities of ~0.6, 1.2 and 5.2S/cm were achieved for ITO nanoparticles synthesized in 0.14, 1.4, 14mol/L ethanolamine, respectively.

The ITO ink synthesized in 14mol/L ethanolamine was chosen to investigate the annealing temperature and ambient atmosphere on the conductivity of ITO film. The deposited ITO films were annealed at different temperatures and ambient conditions, and the results are listed in Table 1. When the annealing was performed at no more than 200°C in air the ITO films did not exhibit high electric conductivity. The conductivity of ITO film was increased sharply by two orders of magnitude when annealing temperature increased from 200 to 300°C in either air or Ar/H_2, in accordance with the weight loss results of ITO nanoparticles (shown in Fig. 7). In this temperature range, ethanolamine, which is chemically adsorbed on ITO nanoparticle surface by MEA-metal chelating, was gradually desorbed and/or decomposed, resulting in decrease of contact resistance between ITO nanoparticles. When the ITO films were annealed at 200 and 300°C in the atmosphere of Ar plus 7.5%H_2 for 2h, their resistivity values decreased to 1.9 and 1.0×10^{-2}Ω·cm, respectively.

To improve the film conductance, spin-coated ITO films were immersed in neutral water (pH=7) to remove surfactant (ethanolamine) from the surface of ITO nanoparticles before annealing. It is well known that hydrolysis of metal-ethanolamine complex would take place and lead to metal hydroxide precipitation if water was added into the metal-ethanolamine complex alcohol solution.[18] Therefore, when immersing spin-coated ITO films in neutral water, metal-ethanolamine on ITO nanocrystals converted into metal hydroxide (as illustrated in Fig. 8a) and ethanolamine dissolved into water. Meanwhile, the ITO nanoparticles lose the

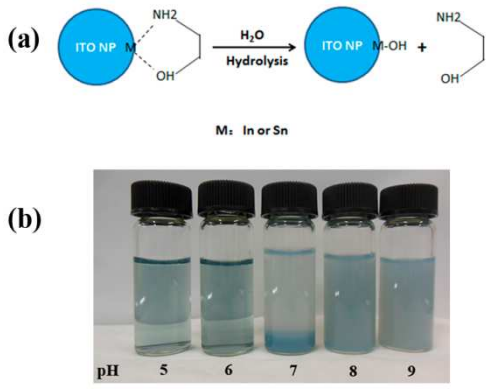

Fig 8 (a) Schematic illustration of conversion of metal-ethanolamine on ITO nanoparticles into metal hydroxide and then the ethanolamine dissolve into the water; (b) ITO suspensions 30min after the addition of water with pH values of 5, 6, 7, 8 and 9 from left to right.

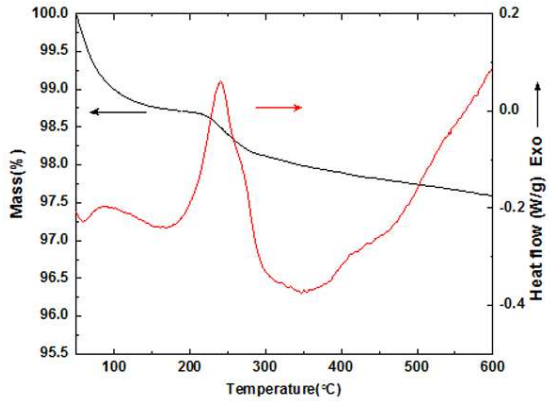

Fig. 9 The TGA-DSC measured in air of the dried precipitate (as show in Fig. 8b) obtained by adding neutral water in ITO ink synthesized with 14mol/L ethanolamine.

good dispersion in liquid phase and would not disperse into water from the substrate. It is important to use water with pH value at 7. Fig. 8b shows the ITO suspensions 30min after the addition of water with pH values of 5, 6, 7, 8 and 9 from left to right. If low pH aqueous liquid is used, ITO will dissolve into metal ion, while high pH value will lead to slow precipitation. TGA-DSC measurement of the precipitate obtained by using pH=7 water are shown in Fig.9. The weight loss in temperature range of 200~300°C was much less than that in fig.7. It confirmed the removal of ethanolamine by the washing process.

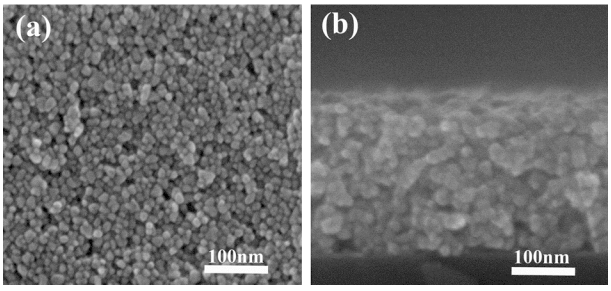

Fig. 10 SEM images of the ITO film: (a) the surface and (b) cross section of the film. The spin-coated film with water washing was annealed at 200 °C under Ar and 7.5% H_2 for 2h.

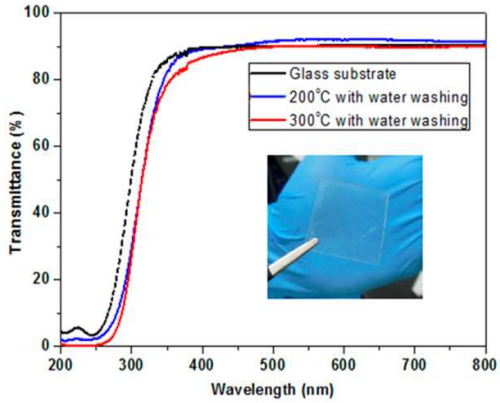

Fig. 11 Transmittance curve of glass and ITO/glass achieved with water washing and annealing under Ar+7.5%H_2 at 200 and 300°C for 2h. The inset pictures show the optical transparency of the ITO/glass annealed at 300°C with water washing.

By immersing the spin-coated ITO films into neutral water before film annealing, the resistivity has reduced to 0.2Ω•cm for ITO film annealed 2h at 200°C and to 8.9×10^{-3}Ω•cm for ITO film annealed 2h at 300°C in the mixed atmosphere of Ar plus 7.5%H_2. The results confirmed that this simple water washing could effectively remove the capping molecules on the surface of ITO nanoparticles to reduce the contact resistance between the nanoparticles. Moreover, high-quality, dense and homogeneous films have been achieved without visible cracks, as the SEM images shown in Fig. 10, while maintaining 90% of high transparency as shown in Fig. 11.

Conclusions

Highly conductive indium tin oxide (ITO) nanocrystals and inks were synthesized by solvothermal dehydration condensation of metal hydroxide in combination with *in-situ* ethanolamine capping. The introduction of ethanolamine effectively reduced the size of nanocrystals and improved their dispersion properties simultaneously. The phenomena were attributed to metal species solubility enhancement and covalent chemically capping effect of ethanolamine, due to its excellent metal chelating activity. The ITO nanocrystals can be well re-dispersed in ethanol to form high solid content (up to 10wt%) suspensions which are stable over days. High-quality conductive ITO films were deposited using the stable suspensions as ink. A water washing process was also introduced after film deposition to get rid of the surface capping agent to improve the film conductivity. ITO films of high transparency (90%) exhibited low resistivity of 8.9×10^{-3} Ω·cm after 2 hours annealing at 300°C in mixed Ar and H_2 atmosphere.

Acknowledgements

This work was supported by the project of the Major Research plan of the Nation Natural Science Foundation of China (Grant No. 91123034), Strategic Priority Research Program of the Chinese Academy of Sciences (Grant No. XDA09020201), and Project supported by National Science and Technology Ministry (Grant No. 2012BAF13B05-402).

Notes and references

Printable Electronics Research Centre, Suzhou Institute of Nano-Tech and Nano-Bionics, Chinese Academy of Sciences, Suzhou, 215123, People's Republic of China, E-mail: zchen2007@sinano.ac.cn, zcui2009@sinano.ac.cn .

1 D. S. Ginley, H. Hosono and D. C. Paine, *Handbook of Transparent Conductors*, Springer-Verlag Berlin, Berlin, Germany, 2010.
2 D. R. Cairns, R. P. Witte, D. K. Sparacin, S. M. Sachsman, D. C. Paine, G. P. Crawford and R. R. Newton, *Applied Physics Letters*, 2000, **76**, 1425-1427.
3 M. Singh, H. M. Haverinen, P. Dhagat and G. E. Jabbour, *Adv. Mater.*, 2010, **22**, 673-685.
4 S. E. Habas, H. A. S. Platt, M. van Hest and D. S. Ginley, *Chem. Rev.*, 2010, **110**, 6571-6594.
5 J. Perelaer, P. J. Smith, D. Mager, D. Soltman, S. K. Volkman, V. Subramanian, J. G. Korvink and U. S. Schubert, *J. Mater. Chem.*, 2010, **20**, 8446-8453.
6 S. Jeong and J. Moon, *J. Mater. Chem.*, 2012, **22**, 1243-1250.
7 N. R. Kim, J. H. Lee, Y. Y. Lee, D. H. Nam, H. W. Yeon, S. Y. Lee, T. Y. Yang, Y. J. Lee, A. Chu, K. T. Nam and Y. C. Joo, *J. Mater. Chem. C*, 2013, **1**, 5953-5959.
8 E. Della Gaspera, M. Bersani, M. Cittadini, M. Guglielmi, D. Pagani, R. Noriega, S. Mehra, A. Salleo and A. Martucci, *J. Am. Chem. Soc.*, 2013, **135**, 3439-3448.
9 L. Luo, D. Bozyigit, V. Wood and M. Niederberger, *Chem. Mat.*, 2013, **25**, 4901-4907.
10 T. Sasaki, Y. Endo, M. Nakaya, K. Kanie, A. Nagatomi, K. Tanoue, R. Nakamura and A. Muramatsu, *J. Mater. Chem.*, 2010, **20**, 8153-8157.
11 G. Buhler, D. Tholmann and C. Feldmann, *Adv. Mater.*, 2007, **19**, 2224.

12 F. Hetsch, N. Zhao, S. V. Kershaw and A. L. Rogach, *Mater. Today*, 2013, **16**, 312-325.
13 J. Lee, S. Lee, G. L. Li, M. A. Petruska, D. C. Paine and S. H. Sun, *J. Am. Chem. Soc.*, 2012, **134**, 13410-13414.
14 J. Lee, M. A. Petruska and S. H. Sun, *J. Phys. Chem. C*, 2014, **118**, 12017-12021.
15 R. Buonsanti and D. J. Milliron, *Chem. Mat.*, 2013, **25**, 1305-1317.
16 G. M. Dalpian and J. R. Chelikowsky, *Phys. Rev. Lett.*, 2006, **96**, 226802.
17 Y. Xia, Y. Xiong, B. Lim and S. E. Skrabalak, *Angewandte Chemie-International Edition*, 2009, **48**, 60-103.
18 L. Znaidi, *Mater. Sci. Eng. B-Adv. Funct. Solid-State Mater.*, 2010, **174**, 18-30.
19 K. Song, Y. Jung, Y. Kim, A. Kim, J. K. Hwang, M. M. Sung and J. Moon, *J. Mater. Chem.*, 2011, **21**, 14646-14654.
20 R. B. H. Tahar, T. Ban, Y. Ohya and Y. Takahashi, *J. Appl. Phys.*, 1998, **83**, 2631-2645.
21 D. Y. Deng, Y. X. Jin, Y. R. Cheng, T. K. Qi and F. Xiao, *Acs Applied Materials & Interfaces*, 2013, **5**, 3839-3846.
22 K. Ankireddy, S. Vunnam, J. Kellar and W. Cross, *J. Mater. Chem. C*, 2013, **1**, 572-579.
23 M. A. Khondoker, S. C. Mun and J. Kim, *Applied Physics a-Materials Science & Processing*, 2013, **112**, 411-418.
24 Y. L. Zhao, L. Duan, G. F. Dong, D. Q. Zhang, J. Qiao, L. D. Wan and Y. Qiu, *Langmuir*, 2013, **29**, 151-157.
25 S. Jeong, J. Y. Lee, S. S. Lee, S. W. Oh, H. H. Lee, Y. H. Seo, B. H. Ryu and Y. Choi, *J. Mater. Chem.*, 2011, **21**, 17066-17070.
26 M. Ohyama, H. Kozuka, T. Yoko and S. Sakka, *J. Ceram. Soc. Jpn.*, 1996, **104**, 296-300.
27 L. Kőrösi, A. Scarpellini, P. Petrik, S. Papp and I. Dékány, *Appl. Surf. Sci.*, 2014, **320**, 725-731.
28 J. N. Nian and H. S. Teng, *J. Phys. Chem. B*, 2006, **110**, 4193-4198.
29 S. Tang, J. Zhang, S. Wu, C. Y. Hu, Y. Li, L. Jiang and Q. L. Cui, *J. Phys. Chem. C*, 2014, **118**, 21170-21176.
30 L. Diamandescu, D. Tarabasanu-Mihaila, M. Feder, M. Enculescu, V. S. Teodorescu, S. Constantinescu, T. Popescu, C. Bartha and Zs. Pap, *Mater. Chem. Phys.*, 2014, **143**, 1540-1549
31 X. Xu and X. Wang, *Inorg. Chem.*, 2009, **48**, 3890-3895.
32 K. H. Seo, J. H. Lee, J. J. Kim, M. I. Bertoni, B. J. Ingram and T.O. Mason, *J. Am. Ceram. Soc.*, 2006, **89**, 3431-3436.
33 V. K. Lamer and R. H. Dinegar, *J. Am. Chem. Soc.*, 1950, **72**, 4847-4854. **000180**

Graphical Abstract

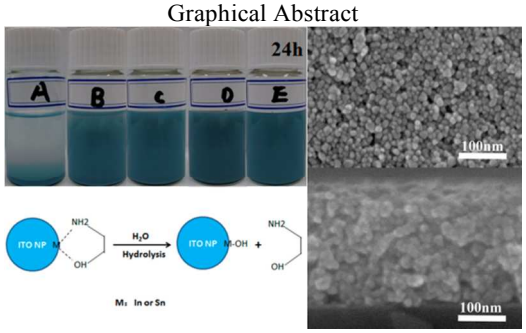

ITO ink are synthesised by addition of different concentration ethanolamine in reaction. A water washing step has been introduced in the ITO film preparation process to improve its conductivity, resulting in low resistivity high-quality films.